Current Limiting Strategy of Grid-forming Converter Based on Additional Current Loop

Jiahui Xi
North China Electric Power University
State Key Laboratory of Alternate Electrical Power System with Renewable Energy Sources
Beijing, China
xijiahui98@163.com

Jinyuan Wang
North China Electric Power University
State Key Laboratory of Alternate Electrical Power System with Renewable Energy Sources
Beijing, China
847090484@qq.com

Jingyi Zhang
Transmission Network Planning Center
State Power Economic Research Institute
Beijing, China
zhangjingyi91@126.com

Yan Zhang
Transmission Network Planning Center
State Power Economic Research Institute
Beijing, China
zhangyan@chinasperi.sgcc.com.cn

Chenbo Su*
North China Electric Power University
State Key Laboratory of Alternate Electrical Power System with Renewable Energy Sources
Beijing, China
scb2636@foxmail.com

Chongru Liu
North China Electric Power University
State Key Laboratory of Alternate Electrical Power System with Renewable Energy Sources
Beijing, China
chongru.liu@ncepu.edu.cn

2022 4th International Conference on Smart Power & Internet Energy Systems (SPIES) | 978-1-6654-8957-7/22/$31.00 ©2022 IEEE | DOI: 10.1109/SPIES55999.2022.10082058

***Abstract*—After the falut of the new energy unit during the grid connection, due to the limited current carrying capacity of the converter, the device will be damaged which can result in the unit off grid operation the grid. In order to solve the above problems, this paper first discusses the main problems existing in the control of existing grid-forming (GFM) converters under grid fault conditions. Then, an additional current control strategy is proposed to control the current components of dq-axis respectively. On the premise of ensuring that the output current of the converter within the allowable range, the proposed strategy guarantees the voltage source characteristics of the converter during the fault period. Finally, the effectiveness and superiority of the proposed control strategy are verified by MATLAB/Simulink simulation.**

***Keywords*—grid-forming converter, current limiting, voltage source characteristics**

I. Introduction

In recent years, under the development background of double carbon policy, the penetration rate of wind power, photovoltaic and other renewable energy connected to the grid through power electronic devices has been continuously improved, which is conducive to changing the classic operation mode of power grid dominated by synchronous motors[1-3]. Compared with the synchronous generator that can withstand up to 7 times its rated current, the converter can only withstand 20%~50% of the overcurrent[4,5]. Therefore, how to suppress the overcurrent during the fault period becomes a key to the normal operation of new energy units.

Grid following (GFL) and grid forming (GFM) can be used for grid connection control of new energy[6-9].GFL has long been regarded as criterion of renewable energy grid connection control. It uses a phase-locked loop to measure the phase of the grid voltage to adjust its power output[10],which only follows the grid angle / frequency. However, GFM can actively controls its frequency and voltage output.

This paper takes the three-phase symmetrical fault with the most serious overcurrent as the scenario, and studies the current limiting strategy of GFM.

This paper is supported by State Grid Science & Technology Project (SGXJJY00GHJS2000091).

At present, the current limiting strategies for overcurrent during short circuit at home and abroad are mainly divided into three types. The first one is to switch to current source mode during fault and directly control current[11-13]. Under this control, the converter presents current source characteristics externally, and can not effectively control the voltage. Therefore, it will cause voltage stability problems during the fault period and recovery period.

The second is the current limiting strategy based on virtual impedance[14,15-17] , according to the difference between the actual current value and the set value, the reference voltage is changed accordingly, that is, equivalent to adding impedance in the circuit. A major problem of this method is the accuracy of current control. The virtual impedance is calculated from the voltage dip and the system loop parameters. The accuracy of the system loop parameters determines the accuracy of current control, and it is difficult to obtain the system loop parameters in actual operation. Another big problem of the virtual impedance is that the inductance current cannot be changed instantaneously, so the existence of the virtual reactance may cause the decaying DC component contained in output current, which will affect the current control effect.

The third is to change the power reference value of the outer power loop[18-19]. In this control mode, the control target is still power, so the accurate control of current cannot be achieved. On the other hand, the response speed is slow because the power reference value acts on the outer loop, and the DC component with larger current at the early stage of fault cannot be suppressed in time.

Aiming at the problems in the existing current limiting strategies, this paper proposes a fault current limiting strategy based on the additional current loop, which still operates as a voltage source during the fault period. The key to this strategy is how to obtain the appropriate reference voltage during the fault, which can not only rapidly limit the overcurrent, but also provide a certain voltage support.

II. Control Strategy of Grid-forming Converter

The control framework of GFM is mainly divided into two parts, which are the outer power loop control loop that calculates the equivalent voltage source angle θ、frequency ω and amplitude u_{dref}, and the inner voltage and current control circuit including all further control actions, finally the modulation signal required by PWM is generated . The control circuit of GFM is shown in Fig. 1. The main circuit includes DC power supply, inverter circuit, LCL filter and grid equivalent circuit.

Each control link will be introduced in detail below.

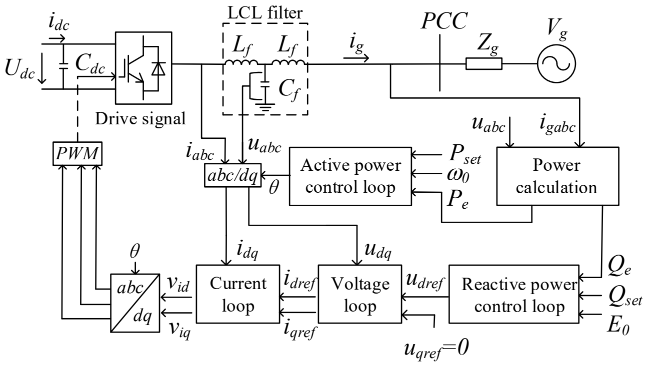

Fig. 1. The main topology and control blocks of the GFM converter

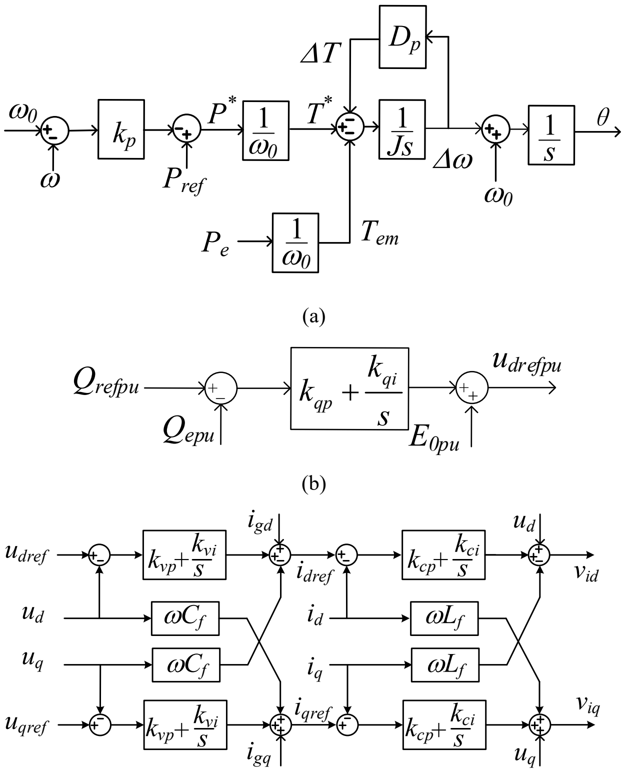

(a)

(b)

(c)

Fig. 2. The detailed structure of main control blocks, (a) The control loop of VSG, (b) The control loop of reactive power, (c) The control loop of current and voltage inner loop

A. Active Power Outer Loop

The active power loop is controlled by VSG. By simulating the synchronous generator governor and rotor motion equation, the operating characteristics similar to synchronous generator can be obtained, which can provide the system with the ability of virtual inertia and synchronous power. The topology of VSG is shown in Fig. 2(a).

Fig. 2(a) shows the control loop of VSG, which mainly simulates the governor and rotor motion equation of generator. The rotor motion equation of the synchronous generator is:

$$J\frac{d^2\theta}{dt^2}=T^*-T_{em}-D_p(\omega-\omega_0) \tag{1}$$

where J is the virtual inertia and D_p is the active damping coefficient. ω_0 is the reference angular velocity, T_{em} is the output torque, which can be expressed as:

$$T_{em}=\frac{P_e}{\omega_0} \tag{2}$$

The reference active power P^* is generated by the governor and can be calculated by the following formula:

$$P^*=P_{ref}-k_p(\omega-\omega_0) \tag{3}$$

where k_p means P-ω coefficient.

From equations (1) - (3):

$$J\frac{d^2\theta}{dt^2}=T_0-T_{em}-D(\omega-\omega_0) \tag{4}$$

where $T_0=P_{ref}/\omega_0$, $D=D_p+k_p/\omega_0$, D means equivalent damping.

B. Reactive Power Outer Loop

The topology of reactive power loop is shown in Fig. 2(b). The reactive power control loop adopts a PI controller to adjust the reactive power Q_e to the set point Q_{ref}. The reference voltage can be calculated by the following formula:

$$v_{dref}(s)=\left(k_{qp}+\frac{k_{qi}}{s}\right)(Q_{ref}-Q_e)+E_0 \tag{5}$$

where k_{qp} and k_{qi} respectively represent the proportional and integral coefficient of PI controller, E_0 and Q_{ref} are the reference voltage and reference reactive power respectively.

C. Current and Voltage Inner Loop

The topology of current and voltage inner loop is shown in Fig. 2(c). To realize voltage oriented control, the voltage component of q-axis is controlled to zero, that is, u_{qref}=0, then the voltage component of d-axis is the voltage amplitude, and the active power and reactive power at PCC point can be expressed as:

$$\begin{cases} P=\frac{3}{2}(u_d i_d+u_q i_q)=\frac{3}{2}u_d i_d \\ Q=\frac{3}{2}(u_q i_d-u_d i_q)=-\frac{3}{2}u_d i_q \end{cases} \tag{6}$$

Therefore, i_q can be used to represent reactive power and i_d can be used to represent active power, that is, the active power loop mainly acts on i_d, and the reactive power loop acts on i_q.

The voltage loop consists of the grid side voltage PI control, dq-axis cross coupling compensation and current feedforward compensation, to realize no static error tracking of the voltage reference value. The output of the voltage loop can be expressed as:

$$\begin{cases} i_{dref}=\left(k_p+\frac{k_i}{s}\right)\left(u_{dref}-u_d\right)-\omega C_f u_q+i_{gd} \\ i_{qref}=\left(k_p+\frac{k_i}{s}\right)\left(u_{qref}-u_q\right)+\omega C_f u_d+i_{gq} \end{cases} \tag{7}$$

where i_{gd} and i_{gq} are dq-axis currents of filter inductors near the grid side, i_{dref} and i_{qref} are the dq-axis current reference value of converter side inductance, u_{dref} and u_{qref} are the dq-axis component reference value of filter capacitor terminal voltage respectively, and u_d and u_q are the actual value of dq-axis voltage across the filter capacitor respectively. k_p and k_i are proportional gain and integral gain of PI controller respectively.

Current loop consists of PI control of inductive current, dq-axis cross coupling compensation and voltage feedforward compensation to realize no static error tracking of current reference value. Its output can be expressed as:

$$\begin{cases} v_{id} = \left(k_p + \frac{k_i}{s}\right)\left(i_{dref} - i_d\right) - \omega L_f i_q + u_d \\ v_{iq} = \left(k_p + \frac{k_i}{s}\right)\left(i_{qref} - i_q\right) + \omega L_f i_d + u_q \end{cases} \quad (8)$$

Where i_d and i_q are the actual values of the dq-axis inductance current. v_{id} and v_{iq} are the signal values output by the current circuit.

III. RESEARCH ON OVERCURRENT SUPPRESSION STRATEGY

The fault current limiting strategy proposed in this paper is mainly realized by the additional current loop, which is divided into two current components of dq-axis, corresponding to active loop and reactive loop respectively.

The setting of active and reactive current components shall refer to the low voltage ride through (LVRT) requirements for wind power grid connection in China[20]. The reference value of dq- axis current during LVRT is given by the following formula:

$$i_{dref} = \begin{cases} i_{d0}, \left(u_d > 0.9\right) \\ \sqrt{I_{\max}^2 - i_{qref}^2}, \left(0.2 \le u_d \le 0.9\right) \end{cases} \quad (9)$$

$$i_{qref} = \begin{cases} 0, \left(u_d > 0.9\right) \\ K_d\left(0.9 - u_d\right) I_N, \left(0.2 \le u_d \le 0.9\right) \end{cases} \quad (10)$$

where, i_{d0} is the reference value of d-axis current before fault, K_d is the gain coefficient of reactive current, which is generally not less than 1.5. Since d-axis voltage orientation is adopted in this paper, u_d is the voltage amplitude of grid connection point, and I_N is the rated current.

A. Active Loop Improvement

Due to the existence of inertia and damping links, VSG can suppress the peak value during frequency fluctuation, but will affect the tracking speed of active power and prolong the time to reach the new stable value[21-22]. Therefore, during the fault period， the response speed is accelerated by reasonably setting the damping coefficient D_p and changing the reference value of active power at the same time. The reference value of active power P'_{ref} during fault can be calculated from the reference value of d-axis current, and its expression is as follows.

$$P'_{ref} = \frac{3}{2} i_{dref} u_{dref} \quad (11)$$

where i_{dref} is the reference value of d-axis current and u_{dref} is the reference value of d-axis voltage during fault.

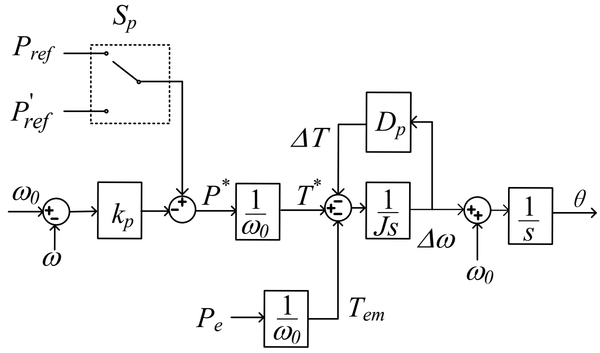

Fig. 3. The improved control loop of VSG

B. Voltage Amplitude Acquisition

During normal operation, the voltage loop control target is the setting value of reactive power, and the voltage reference value is generated through the reactive outer loop. During the fault period, the control target of the strategy proposed in this paper is the setting value of q-axis current. The additional current loop is used to calculate the voltage reference value. In case of fault, the switch S_q is open, S_{PIq} is closed, and the reference voltage is given by the additional current loop. The control block diagram is as follows.

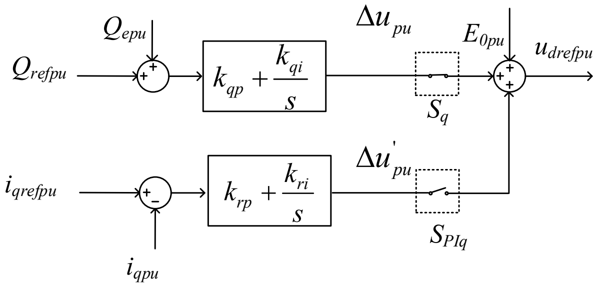

Fig. 4. The control of voltage amplitude

IV. CALCULATION AND SIMULATION ANALYSIS

The simulation in this paper is carried out in Matlab/Simulink environment to test and verify the effectiveness of the proposed control strategy. The system parameters are shown in Table I. In order to simulate the power grid fault, the power grid equivalent voltage v_g in Fig. 1 is directly controlled. In this paper, the three-phase short-circuit fault occurs in the system when t=0.3s, and the fault is removed when t=0.7s. The simulation duration is 1.2s, and the overcurrent limit of the converter is set to 1.5pu.

TABLE I. PARAMETERS OF SIMULATION SYSTEM

Project	Numerical value
Frequency reference f_0 (Hz)	50
Voltage amplitude reference E_0 (V)	690
DC Bus Voltage V_{dc} (V)	1200
Converter side inductance L_{cf} (mH)	1.5
Filter capacitance C_f (μF)	30

Project	Numerical value
Grid side inductance L_g (H)	1
Line resistance R_L (Ω)	0.3
Line inductance L_L (mH)	0.4
Base power S_n (kVA)	30

The current restraining effect and system characteristics of new energy units under the original control (OC) and the additional current control (ACC) proposed in this paper will be compared and analyzed as follows.

A. Comparison and Analysis of Active Output

Taking the serious fault in which the grid voltage drops to 0.2 pu as an example, under the original control strategy, the active reference value remains unchanged, and the active reference value is given by the droop link of the analog governor. According to the active output curve in Fig. 5, due to the existence of VSG inertia and damping link, the response speed is slow, so the active output cannot be stable quickly. The additional current control greatly accelerates the adjustment speed of active power and achieves stability within 0.1s by changing the reference value of active power during the fault period.

It can be seen from the reactive power output curve in Fig. 5 that the additional current control can quickly provide stable reactive power for the system to maintain the voltage stability of the PCC point due to its good dynamic response.

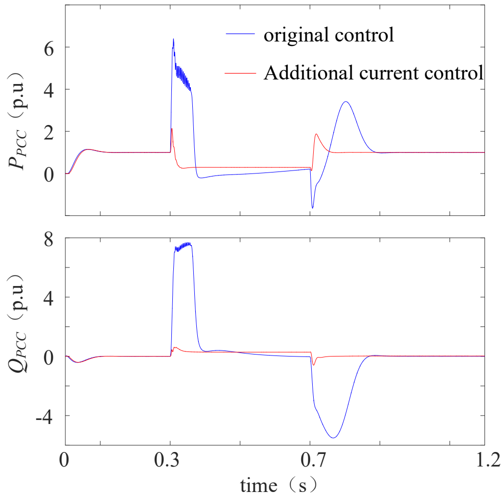

Fig. 5. The comparison of transmission power

B. Comparative Analysis of Voltage and Current

Taking the serious fault in which the grid voltage drops to 0.2 pu as an example, Fig. 6 and Fig. 7 respectively show the comparison of output current dq-axis component and three-phase current waveform under the original control and the proposed control. Through the comparison, it can be seen that under the original control, due to the slow response speed, the overcurrent at the early stage of the fault cannot be suppressed in time. When the grid voltage drops to 0.2 pu, the converter will suffer a continuous overcurrent of more than 10 pu, which will damage the grid connected power electronic devices and lead to unit disconnection. The proposed control responds quickly after system fault and stabilizes the output current at the set value within 0.1s.

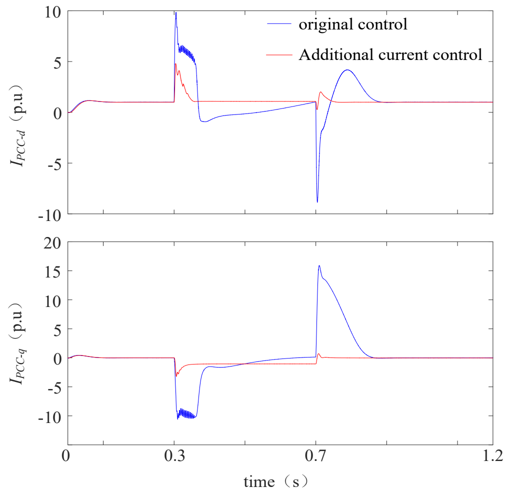

Fig. 6. The comparison of dq- axis current component

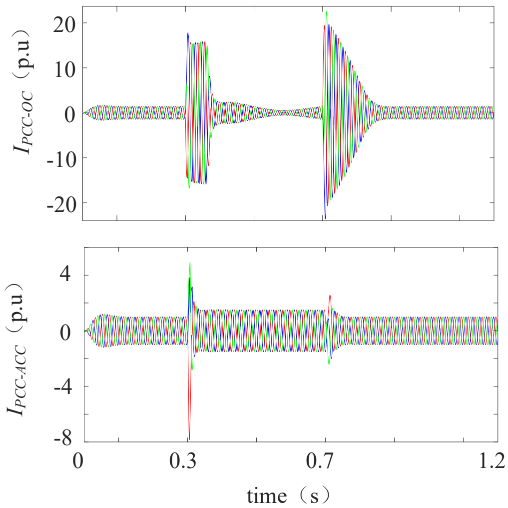

Fig. 7. The comparison of output current

Fig. 8 shows the comparison of the voltage amplitude of PCC point under the original control and the proposed control. Through the comparison, it can be seen that the external loop reactive reference value under the original control is not suitable for the operation during the fault period, so that the appropriate reference voltage cannot be generated, and the voltage cannot be quickly stabilized due to the untimely response of the external loop. It can be seen that within 0.1s after the fault, the additional current control acts quickly to generate an appropriate reference voltage, and then the converter operates as a voltage source, which can provide higher and more stable voltage support for PCC point compared with the original control.

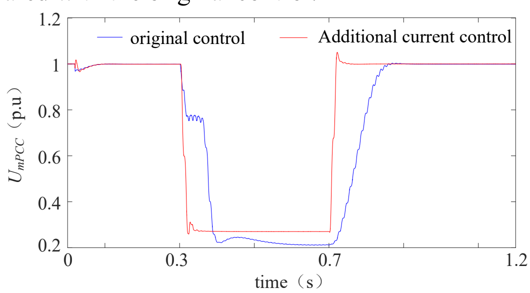

Fig. 8. The comparison of voltage amplitude at PCC point

V. CONCLUSION

Aiming at the overcurrent problem caused by three-phase symmetrical fault in the system, this paper summarizes the problems of current suppression speed, voltage stability in the existing current limiting strategy, and proposes an additional current loop control method. The following conclusions are obtained:

(1) After the three-phase symmetrical short-circuit fault occurs in the power grid, due to the GFM characteristics, the current reacts quickly to provide reactive current support for the power grid;

(2) After switching to the additional current control during the fault period, the fault current quickly stabilizes at the set value. At the same time, it ensures the voltage source characteristics of GFM and provides continuous and stable voltage support for the power grid;

(3) The proposed strategy makes full use of the converter capacity margin to ensure the active power transmission capacity during fault while providing reactive power support;

Finally, the effectiveness of the proposed control strategy is verified by Matlab/Simulink simulation.

REFERENCES

[1] H. L. R., C. Z. and P. D., "Grid-Forming Inverters: A Critical Asset for the Power Grid," IEEE Journal of Emerging and Selected Topics in Power Electronics, vol. 8, pp. 925-935, 2020-01-01 2020.

[2] B. L. N., M. L., T. A., N. B. G., and R. P., "Frequency Selective Damping of Sub-synchronous Oscillations for Grid-Forming Power Converters," in 2021 IEEE Energy Conversion Congress and Exposition (ECCE), 2021, pp. 877-881.

[3] D. W., C. Z., P. S. K., H. L. R., P. N. S., K. T. F., and K. S., "A Comparative Study of Two Widely Used Grid-Forming Droop Controls on Microgrid Small-Signal Stability," IEEE Journal of Emerging and Selected Topics in Power Electronics, vol. 8, pp. 963-975, 2020-01-01 2020.

[4] S. Z., H. W., S. C., G. J., and J. S. Z., "Characteristics and Restraining Method of Fast Transient Inrush Fault Currents in Synchronverters," IEEE Transactions on Industrial Electronics, vol. 64, pp. 7487-7497, 2017-01-01 2017.

[5] Q. T., G. F., C. F., D. G., P. T., and G. X., "Critical Clearing Time Determination and Enhancement of Grid-Forming Converters Embedding Virtual Impedance as Current Limitation Algorithm," IEEE Journal of Emerging and Selected Topics in Power Electronics, vol. 8, pp. 1050-1061, 2020-01-01 2020.

[6] L Huang, H Xin, P Ju,et al, "Synchronous stability analysis and unified synchronous control structure of power electronic grid connected equipment ," Power Automation Equipment, vol. 40, pp. 10-25, 2020.

[7] Y Cen, "Research on impedance modeling and voltage tracking capability of grid connected converter based on phase locked synchronization , ":Wuhan University, 2018.

[8] P. D., H. L. R. and M. J. T., "Comparison of Grid Following and Grid Forming Control for a High Inverter Penetration Power System," in 2018 IEEE Power & Energy Society General Meeting (PESGM), 2018, pp. 1-5.

[9] R. R., W. X., L. M., L. X., and E. S., "Grid-Forming Converters: Control Approaches, Grid-Synchronization, and Future Trends—A Review," IEEE Open Journal of Industry Applications, vol. 2, pp. 93-109, 2021-01-01 2021.

[10] A. T., P. T., V. V., J. R. A., M. J., and M. N., "Paving the Way: A Future Without Inertia Is Closer Than You Think," IEEE Power and Energy Magazine, vol. 15, pp. 61-69, 2017-01-01 2017.

[11] S. I., E. H. G. M., M. G. J., and M. A., "A Current Limiting Strategy to Improve Fault Ride-Through of Inverter Interfaced Autonomous Microgrids," IEEE Transactions on Smart Grid, vol. 8, pp. 2138-2148, 2017-01-01 2017.

[12] M. Yu, W. Huang, N. Tai, X. Zheng, P. Wu, and W. Chen, "Transient stability mechanism of grid-connected inverter-interfaced distributed generators using droop control strategy," Applied Energy, vol. 210, pp. 737-747, 2018.

[13] C. Z. Q. and C. K. G., "Current-Limiting Droop Control of Grid-Connected Inverters," IEEE Transactions on Industrial Electronics, vol. 64, pp. 5963-5973, 2017-01-01 2017.

[14] D. P. A. and M. D. D., "Virtual Impedance Current Limiting for Inverters in Microgrids With Synchronous Generators," IEEE Transactions on Industry Applications, vol. 51, pp. 1630-1638, 2015-01-01 2015.

[15] H. J. and W. L. Y., "Analysis, Design, and Implementation of Virtual Impedance for Power Electronics Interfaced Distributed Generation," IEEE Transactions on Industry Applications, vol. 47, pp. 2525-2538, 2011-01-01 2011.

[16] H. M., F. Y., O. T., and F. T., "An Operating Mode of Voltage Source Inverter for Fault Current Limitation," in Proceedings of the 41st International Universities Power Engineering Conference, 2006, pp. 598-602.

[17] W. L. Y., M. V. D., C. L. P., and B. F., "A Dual-Functional Medium Voltage Level DVR to Limit Downstream Fault Currents," IEEE Transactions on Power Electronics, vol. 22, pp. 1330-1340, 2007-01-01 2007.

[18] A. E., R. M. G., R. R., F. B., Y. Y., B. F., and F. S., "Control Strategy for Three-Phase Grid-Connected PV Inverters Enabling Current Limitation Under Unbalanced Faults," IEEE Transactions on Industrial Electronics, vol. 64, pp. 8908-8918, 2017-01-01 2017.

[19] G. T. M., W. X., D. P., and B. F., "Current Limiting Control With Enhanced Dynamics of Grid-Forming Converters During Fault Conditions," IEEE Journal of Emerging and Selected Topics in Power Electronics, vol. 8, pp. 1062-1073, 2020-01-01 2020.

[20] China Electric Power Research Institute, "Technical Regulations on Wind Farm Connection to Power System," :General Administration of Quality Supervision, Inspection and Quarantine of the People's Republic of China; China National Standardization Administration.

[21] Q Qin, "Research on microgrid control strategy and islanding detection based on virtual synchronous generator, ":Harbin Institute of technology, 2021

[22] Z Lan, Y Long, J Ceng,et al, " Transient power oscillation suppression strategy of virtual synchronous generator considering overshoot, " Power System Automation, vol.46,pp. 131-141,2022.